Trabecular network arrangement within the human patella – how osteoarthritis remodels the 3D trabecular structure

Sebastian Hoechel

Department of Biomedicine, Musculosceletal Research, University of Basel, Pestalozzistrasse 20, 4056 Basel, Switzerland

Hans Deyhle

Biomaterials Science Center, University of Basel, Gewerbestrasse 14, 4123 Allschwil, Switzerland

Mireille Toranelli

Department of Biomedicine, Musculosceletal Research, University of Basel, Pestalozzistrasse 20, 4056 Basel, Switzerland

Magdalena Müller-Gerbl

Department of Biomedicine, Musculosceletal Research, University of Basel, Pestalozzistrasse 20, 4056 Basel, Switzerland

Supported by the Swiss National Science Foundation (Grant 316030_133802/1)

ABSTRACT

Following the principles of "morphology reveals biomechanics", the anatomical structure of the cartilage-osseous interface and the supporting trabecular network show defined adaptation in their architectural properties to physiological loading. In case of a faulty relationship, the ability to support the load diminishes and the onset of osteoarthritis (OA) may arise and disturb the balanced formation and resorption processes. To describe and quantify the changes occurring, 10 human OA patellae were analysed concerning the architectural parameters of the trabecular network within the first five mms by the evaluation of 3Dmicro-CT datasets.

The analysed OA-samples showed a strong irregularity for all trabecular parameters across the trabecular network, no regularity in parameter distribution was found. In general, we saw a decrease of material in the OA population as BV/TV, BS/TV, Tb.N and Tb.Th were decreased and the spacing increased. The development into depth showed a logarithmic dependency, which revealed the greatest difference for all parameters within the first mm in comparison to the physiologic samples. The differences decreased towards the 5^{th} mm. The interpretation of the mathematic dependency leads to the conclusion that the main impact of OA is beneath the subchondral bone plate (SBP) and lessens with depth. Next to the clear difference in material, the architectural arrangement is more rod-like and isotropic just beneath the SBP in comparison to the plate-like and more anisotropic physiological arrangement.

Key words: Osteoarthritic human patella, Subchondral bone, Trabecular architecture, Micro-computed tomography

Developments in X-Ray Tomography X, edited by Stuart R. Stock, Bert Müller, Ge Wang, Proc. of SPIE Vol. 9967, 99670M · © 2016 SPIE · CCC code: 0277-786X/16/$18 · doi: 10.1117/12.2237045

1 INTRODUCTION

As the largest sesamoid bone of the human body, the patella centralizes the divergent forces deriving from the 4 heads of the quadriceps muscle and increases their functional lever arm by transmitting the generated force across the knee to the patellar tendon and tibial tuberosity at a greater distance from the axis of rotation. In the movement of sliding along the femoral condyles, the hyaline articular cartilage provides an aneural and frictionless thick tissue that is specifically adapted to the bearing of high compressive loads [1, 2]. Additionally, it functions as a bony shield for the trochlea and the femoral condyles while the knee is in flexion [3].

Since the tibia rotates laterally during the knee extension process, the tibial tubercle, as the insertion point for the patellar ligament, becomes laterally displaced. The so created quadriceps angle between the line of application of the quadriceps force and the direction of the patellar tendon produces a lateral displacement vector of the patella on the frontal plane [4]. In consequence, the contact area of the lateral patellar facet with the lateral femoral condyle within this patellofemoral joint (PFJ) is about 60% greater than on the medial side. The vector also leads to a consistently greater contact force on the lateral facet of the patella [5-8].

This biomechanical situation within the PFJ accounts for the specific anatomical structure of the knee cap as a response. As studies on physiologic human patellae revealed, a predominant maximum of density on the lateral facet of the articular surface of the patella can be found. The described maximum decreases peripherally but shows extensions over the vertical ridge in between both facets onto the medial side. Furthermore, Eckstein at al. [9] showed a constant maximum in cartilage thickness on the lateral facet which correlates with the described density distribution. These regular and reproducible distribution patterns of both mineralization of the subchondral bone plate (SBP) and its cartilage thickness can be seen as an adaption of the locomotor system to long-term load intake in regards to the ideas of Julius Wolff.

In literature, this expression of “Wolff’s law” was incipiently discussed by Ficat and Hungerford in 1977 [10]. They described the sheets of trabecular bone as more or less parallel to each other but perpendicular to the coronal plane of the patella and therefore slightly oblique vis-à-vis the articular facets. The described results are interpreted as an architectural behaviour in dependence to the applied tensile forces and to ideally meet the mechanical demands. At about the same time, Raux et al. also worked on the trabecular architecture of the human patella [11]. Their analysis of microradiographs, derived from sagittal and horizontal cuts, went one step further and firstly described a sheet-and-rod model. Here, orientated sheets of bony tissue which accounted for trabeculae were connected laterally by rods. The lamellae on the lateral facet are described to be more parallel and orientated than on the medial one, which, in its systematic manner, is descripted as response to the biomechanical demands of the patella.

Next to the common differences in trabecular architecture as function of anatomic position, loading direction and load accumulation over time [12, 13], precise correlations to individual long-term load intake are described [14, 15]. In case of a faulty relationship between the loading in a joint and the ability of its components to support the load, the pathogenesis of osteoarthritis (OA) as a disease of the whole joint may arise [16, 17]. Whether the primary lesion occurs in the cartilage or SBP, models of induced arthritis led to subchondral bone changes where subsequent trabecular remodelling results in less compliant trabecular bone and therefore excessive stress in the overlying articular cartilage [18, 19].

The resulting impairments of the trabecular network in OA have quantitatively been described to be higher in bone volume due to an uncoupled balance between resorption and formation, whether through an increase in trabecular number and a reduced spacing or a simple thickening of trabecular.

Since the method of 3D analysis using micro-Ct-data can reveal data of the whole of the trabecular structure without mathematical interpolation and assumptions, we aimed to:

(I) Evaluate the trabecular architecture of OA patellae
    a. Beneath the entire SBP to achieve a demonstration of the regional distribution
    b. In 1 mm steps (layers), starting just beneath the SBP to a depth of 5 mms to describe the development;
(II) Compare the findings to healthy samples.

2 MATERIAL AND METHODS

2.1 Material

Ten human patellae from different individuals were used (5 male, 5 female; age 60 – 74 years, mean 69.4). The inclusion criterion was cartilage degeneration (Outerbridge classification Grade IV) on the medial and lateral facet.
In consideration of The Code of Ethics of the World Medical Association (Declaration of Helsinki) for experiments involving humans, the samples were taken from body-donors to the Department of Anatomy, University of Basel, who contributed their body to science and research only.

2.2 Methods

Micro-CT measurements
µCT experiments were performed with the phoenix nanotom® m holding the patella in a polyethylene container filled with fixation solution to prevent the tissue from drying. The samples were scanned with a cone-beam device with micro-focus tube using 3D metrology (acceleration voltage: 140 kV; beam current; 60 µAs; 0.1 mm aluminum-filter). The. 2100 projections (exposure time: 0.5 s) were recorded over 360 degrees, defining the resulting isotropic pixel size of 32 µm, isotropic. The resulting 3D dataset is based on a modified Feldkamp algorithm [20].
In accordance to a previous conducted study on healthy patellae, the 3D datasets of the patellae were divided into 24 measuring cubes (8 mm x 8 mm x SBP to anterior cortical bone) by the use of the visualization and analysis software VGStudio® Max 2.2 (Heidelberg, Germany). In a first step, the thickness of the subchondral bone plate was evaluated. Following, the trabecular bone of the first five mms (1st ROI: 0-1 mm of trabecular bone below the SBP, 2nd ROI: 1-2 mm, likewise for the 3rd, 4th, and 5th ROI) beneath the SBP of the produced measuring cubes was analysed with the help of the Skyscan software CT-analyser® (Bruker-Microct, Belgium) [14] (Fig.1).
The obtained parameters of bone histomorphometry and architecture were selected according to literature recommendations of bone analysis [21-24].

Obtained parameters for analysis

In accordance to literature and the described main parameters of trabecular bone architecture:

a. BV/TV, (%); indices of bone volume (BV) in relation to the total volume (TV);
b. BS/TV, (1/mm); bone surface density (BS) in relation to the total volume (TV);
c. Tb.Th, (mm); parameter of dimension for the trabecular thickness; and
d. Tb.Sp, (mm); trabecular separation;

as primary measurements in bone histomorphometry [22].

Derived indices:

e. Tb.N, (1/mm); the trabecular number;

as structural parameter [22, 24].

As well as:

f. SMI, (dimensionless); the structure model index; and
g. DA, (dimensionless); the degree of anisotropy;

to directly quantify the otherwise subjective classification of plate-like and rod-like trabecular architecture and to assess the 3D symmetry of it [23].

2.3 Statistical analysis

Depth based data analysis was performed for every measuring cube. The presented data was analysed regarding each patella. The results are seen in relation to the data collected on a healthy sample population [14].

Statistical analysis included the Pearson product-moment correlation coefficient, a two-tailed *t*-test stating the significance as well as the Kolmogorov-Smirnov test for evaluation of the distribution level of the data. All analyses were done using RStudio (RStudio: Integrated-development environment for R, Version 0.99.467, Boston, MA, USA).

3 RESULTS

3.1 Trabecular measurements of OA Patellae

The OA population revealed no noticeable distribution pattern. Multi-side maxima and minima of all analysed parameters were present. Still, BV/TV, BS/TV, Tb.Th and Tb.N showed a steady decrease of absolute value into depth, where the decrease of the absolute parameter value per mm of depth declined with depth showing the largest differences between the 1st and 2nd mm. This steady but declining decrease and therefore the development of each of the parameters into depth could be described as logarithmic dependency. As for Tb.Sp, SMI and DA, an ongoing increase was seen. Here as well the increase was the most in between the first and the second mm and reduced towards the difference between the 4th and 5th mm. The dependency of these parameters was also mathematically described and revealed a logarithmic dependency (Tab. 1).

3.2 Comparrison to physiological population

The trabecular parameters of the OA sample population showed in comparison no defined distribution pattern in regards to the physiological long-term load intake. Multiple maxima and minima without reproducible pattern were present which nevertheless showed a consistency into depth. Still, BV/TV, BS/TV, Tb.Th. and Tb.N showed significant ($p<0.1$) lower values in the OA group in every analysed depth. The difference of absolute value in each layer declined into the depth, showing the largest absolute differences in the 1st, the smallest differences in the 5th mm. BV/TV's absolute difference in the 5th mm was 55.8% of the first mm (Tbl. 1), Tb.Th. 77.8% and Tb.N 63.1%. In addition, the percentage of the absolute difference in regards to the absolute value of the physiological sample reduced in depth (Tab.1, 6th column). Tb.Sp, DA and SMI revealed significant ($p<0.1$) higher values in the OA sample population. Here as well, the difference of the absolute parameter value in comparison to the healthy sample population decreased with depth and revealed the smallest difference in the 5th mm (Tab. 1).

4 DISCUSSION

Even though OA is regarded a disease of the whole joint with a multifactorial aetiology, excessive pressure is at the base and responsible for all conflicts leading to arthrosis. It may result from ligament derangements, deformities or congenital soft tissue anomalies, which all result in mechanical factors to evolve the destructive cascade of this disease [16, 17]. As result, the dynamic state of destructive forces and repair mechanisms impair the homeostasis of the joint [25].

Following the lateral vector force of the quadriceps muscle as well as the predominance of the lateral patello-femoral joint, the lateral compartment arthrosis of the patello-femoral joint is by far more common than its medial counterpart [26]. Before anterior-posterior X-ray show static deformities like osteophyte formation or joint line narrowing, the turning point of the degeneration of the articular cartilage has already passed.

As for the patella, the chondromalacia or cartilage softening of the lateral facet follows secondary to an excessive pressure syndrome, for the medial compartment a non-physiological combination of compression and shear stress. In the end, this loss of elasticity, which the cartilage softening induces, decreases the functional ability of pressure distribution of the articular cartilage and leads to a reaction of adjacent of the SBP to which the articular forces are transferred

abnormally [10]. Following previous studies of the adaptation of the SBP to long-term load intake, this irregular distribution would result in an abnormal density distribution pattern as it is not seen in physiologic samples. The constant maximum of density and therefore calcium hydroxyapatite deposition on the lateral facet of the patella as it has been described before was here not present [27, 28]. Instead, the deposition was spot-like scattered over the entire joint surface, describing a long-term load intake, which is not in correlation to the physiologically applied pressure. In between the spots of high density, lacunae of very low concentration were present.

Since the changes within the cartilage-osseous interface leads to alterations of the pressure distribution and transfer into the trabecular bone system, differences of the 3D network in comparison to the non-pathological situation demonstrating the bone turnover associated with OA are expected.

In contrast to studies using bone-cores or cuts from selected areas of OA degenerated bones, we acquired data of the whole trabecular network of pathological patellae for the comparison with a healthy sample collection. Therefore, our data cannot be seen as selective measurement resembling the architectural situation of the whole of the trabecular network, but actually includes the whole of the first 5 mms under the SBP in volume where the main differences and changes are reported to happen [29]. Given this fact, one has to be careful to compare absolute numerical results to previous published data but has to focus on the general statements about the differences of healthy and OA.

In general, we saw a decrease of material in the OA population as the bone volume as well as the trabecular number and thickness decreased and the spacing was significantly wider ($p < 0.1$). These results correlate with the study of Dedrick et al., who showed a reduced Tb.Th in severe OA as well as Ding et al. who also demonstrated a decrease in trabecular bone structure and mechanical properties [30, 31]. Newly published results of an anterior cruciate ligament transection model in a rabbit model also demonstrated significant reduction of BV/TV and Tb.Th in the medial femoral compartment of the OA knee [32].

Overall, this study substantiates and enlarges the results of Patel et al. published in 2003 [29].

Like us, they describe the BV/TV and Tb.Th to be lower in the OA samples with SMI and Tb.Th to be higher. Tb.N showed no significant variation, whereas in the patella, we saw a significant reduction in the OA sample collection. The development into depth is plotted, but not described in detail. We, for this point, found a logarithmic dependency which interestingly showed the greatest difference for all parameters within the first mm, decreasing towards the 5th.

In conclusion, the main impact of OA is beneath the SBP and lessens with depth. Next to the clear distinction of less material within the 1st mm of trabecular bone, the architectural arrangement reveals to be more rod-like and isotropic just beneath the SBP in OA in comparison to the plate-like and more anisotropic physiological arrangement. Clearly, the alteration in pressure distribution leads to a change in trabecular architecture which is more severe just beneath the SBP than in deeper areas where the pressure is already more homogenously distributed.

5 REFERENCES

1. Aglietti P, Buzzi R, Insall J. Disorders of the patellofemoral joint. Surgery of the knee. 2001;1:913-1043.
2. HUNGERFORD DS, BARRY M. Biomechanics of the patellofemoral joint. Clinical orthopaedics and related research. 1979;144:9-15.
3. Scuderi GR. The patella: Springer Science & Business Media; 1995.
4. Fox AJ, Wanivenhaus F, Rodeo SA. The basic science of the patella: structure, composition, and function. Journal of Knee Surgery. 2012;25(2):127.
5. HEHNE H-J. Biomechanics of the patellofemoral joint and its clinical relevance. Clinical orthopaedics and related research. 1990;258:73-85.
6. Hefzy M, Jackson W, Saddemi S, Hsieh Y-F. Effects of tibial rotations on patellar tracking and patello-femoral contact areas. Journal of biomedical engineering. 1992;14(4):329-43.
7. Fitzpatrick CK, Baldwin MA, Ali AA, Laz PJ, Rullkoetter PJ. Comparison of patellar bone strain in the natural and implanted knee during simulated deep flexion. Journal of Orthopaedic Research. 2011;29(2):232-9.
8. Borotikar B, Sheehan F. In vivo patellofemoral contact mechanics during active extension using a novel dynamic MRI-based methodology. Osteoarthritis and Cartilage. 2013;21(12):1886-94.
9. Eckstein F, Muller-Gerbl M, Putz R. Distribution of subchondral bone density and cartilage thickness in the human patella. Journal of anatomy. 1992 Jun;180 (Pt 3):425-33.
10. Ficat RP, Hungerford DS. Disorders of the patello-femoral joint: Williams & Wilkins Baltimore; 1977.
11. Raux P, Townsend PR, Miegel R, Rose RM, Radin EL. Trabecular architecture of the human patella. Journal of biomechanics. 1975 Jan;8(1):1-7.
12. Evans FG, King AI. Regional differences in some physical properties of human spongy bone. Biomechanical studies of the musculo-skeletal system: Charles C. Thomas Springfield, IL; 1961. p. 19-67.
13. Goldstein SA. The mechanical properties of trabecular bone: dependence on anatomic location and function. Journal of biomechanics. 1987;20(11):1055-61.
14. Hoechel S, Schulz G, Müller-Gerbl M. Insight into the 3D-trabecular architecture of the human patella. Annals of Anatomy-Anatomischer Anzeiger. 2015;200:98-104.
15. Nowakowski AM, Deyhle H, Zander S, Leumann A, Müller-Gerbl M. Micro CT analysis of the subarticular bone structure in the area of the talar trochlea. Surgical and Radiologic Anatomy. 2013;35(4):283-93.
16. Sun HB. Mechanical loading, cartilage degradation, and arthritis. Annals of the New York Academy of Sciences. 2010;1211(1):37-50.
17. Valderrabano V, Horisberger M, Russell I, Dougall H, Hintermann B. Etiology of ankle osteoarthritis. Clinical Orthopaedics and Related Research®. 2009;467(7):1800-6.
18. Radin EL, Parker HG, Pugh JW, Steinberg RS, Paul IL, Rose RM. Response of joints to impact loading—III: Relationship between trabecular microfractures and cartilage degeneration. Journal of biomechanics. 1973;6(1):51-7.

19. Burr DB, Martin RB, Schaffler MB, Radin EL. Bone remodeling in response to in vivo fatigue microdamage. Journal of biomechanics. 1985;18(3):189-200.
20. Feldkamp L, Davis L, Kress J. Practical cone-beam algorithm. JOSA A. 1984;1(6):612-9.
21. Dempster DW, Compston JE, Drezner MK, et al. Standardized nomenclature, symbols, and units for bone histomorphometry: a 2012 update of the report of the ASBMR Histomorphometry Nomenclature Committee. Journal of bone and mineral research. 2013;28(1):2-17.
22. Hildebrand T, Laib A, Muller R, Dequeker J, Ruegsegger P. Direct three-dimensional morphometric analysis of human cancellous bone: microstructural data from spine, femur, iliac crest, and calcaneus. J Bone Miner Res. [Research Support, Non-U.S. Gov't]. 1999 Jul;14(7):1167-74.
23. Hildebrand T, Ruegsegger P. Quantification of Bone Microarchitecture with the Structure Model Index. Comput Methods Biomech Biomed Engin. 1997;1(1):15-23.
24. Parfitt AM, Drezner MK, Glorieux FH, et al. Bone histomorphometry: standardization of nomenclature, symbols, and units: report of the ASBMR Histomorphometry Nomenclature Committee. Journal of bone and mineral research. 1987;2(6):595-610.
25. Helminen H, Jurvelin J, Kiviranta I, Paukkonen K, Saamanen A, Tammi M. Joint loading effects on articular cartilage: a historical review. Joint Loading: Biology and Health of Articular Structures. 1987:1-46.
26. CASSCELLS SW. Gross pathological changes in the knee joint of the aged individual: a study of 300 cases. Clinical orthopaedics and related research. 1978;132:225-32.
27. Hoechel S, Wirz D, Muller-Gerbl M. Density and strength distribution in the human subchondral bone plate of the patella. International orthopaedics. 2012 Sep;36(9):1827-34.
28. Muller-Gerbl M. The subchondral bone plate. Adv Anat Embryol Cell Biol. [Review]. 1998;141:III-XI, 1-134.
29. Patel V, Issever AS, Burghardt A, Laib A, Ries M, Majumdar S. MicroCT evaluation of normal and osteoarthritic bone structure in human knee specimens. Journal of Orthopaedic Research. 2003;21(1):6-13.
30. Dedrick DK, Goldstein SA, Brandt K, O'Connor B, Goulet RW, Albrecht M. A longitudinal study of subchondral plate and trabecular bone in cruciate-deficient dogs with osteoarthritis followed up for 54 months. 1993.
31. Ding M, Hvid I. Quantification of age-related changes in the structure model type and trabecular thickness of human tibial cancellous bone. Bone. 2000;26(3):291-5.
32. Florea C, Malo M, Rautiainen J, et al. Alterations in subchondral bone plate, trabecular bone and articular cartilage properties of rabbit femoral condyles at 4 weeks after anterior cruciate ligament transection. Osteoarthritis and Cartilage. 2015;23(3):414-22.

6 FIGURES AND TABLES

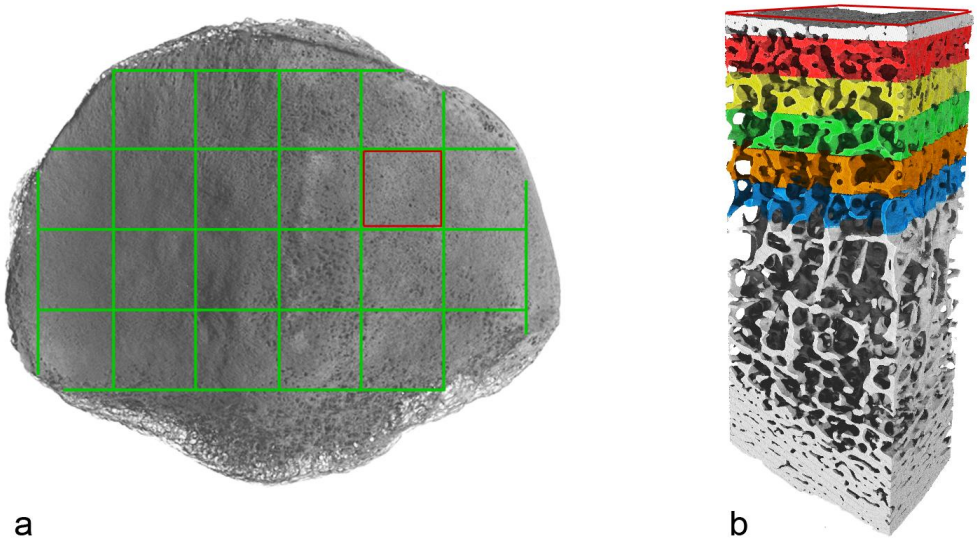

Figure 1 Method of µ-CT; definition of measuring cube and regions of interest; a) 3D reconstruction, patella in dorsal view, 24 measurement cubes marked, b) Measurement cube with 5x1 mm region of interest (1st ROI: red; 2nd ROI: yellow; 3rd ROI: green; 4th ROI: orange; 5th ROI: blue) just below the subchondral bone plate

Bone parameter	Loc.	physiol ■	OA ▲	Absolut diff.	% diff. of physiol
BV/TV (%)	0-1 mm	37.39	25.03	12.37	33.08
	1-2 mm	30.65	20.79	9.87	32.20
	2-3 mm	26.96	18.35	8.61	31.94
	3-4 mm	24.93	17.23	7.69	30.85
	4-5 mm	23.41	16.51	6.90	29.47
BS/TV (1/mm)	0-1 mm	6.65	5.64	1.01	15.15
	1-2 mm	5.96	5.03	0.93	15.64
	2-3 mm	5.52	4.66	0.86	15.66
	3-4 mm	5.21	4.42	0.79	15.11
	4-5 mm	5.02	4.27	0.75	14.94
Tb.Th (mm)	0-1 mm	0.19	0.17	0.03	13.29
	1-2 mm	0.18	0.16	0.02	12.86
	2-3 mm	0.17	0.15	0.02	12.09
	3-4 mm	0.17	0.15	0.02	12.17
	4-5 mm	0.17	0.15	0.02	11.83
Tb.Sp (mm)	0-1 mm	0.36	0.43	0.06	17.85
	1-2 mm	0.41	0.46	0.05	11.58
	2-3 mm	0.44	0.48	0.04	9.47
	3-4 mm	0.46	0.50	0.04	8.02
	4-5 mm	0.48	0.51	0.03	6.97
Tb.N (1/mm)	0-1 mm	1.91	1.47	0.44	23.20
	1-2 mm	1.67	1.29	0.38	22.89
	2-3 mm	1.54	1.19	0.35	22.96
	3-4 mm	1.44	1.13	0.31	21.48
	4-5 mm	1.37	1.09	0.28	20.40
SMI	0-1 mm	0.75	1.28	0.54	71.75
	1-2 mm	1.02	1.42	0.40	39.43
	2-3 mm	1.14	1.51	0.36	31.69
	3-4 mm	1.24	1.55	0.31	24.66
	4-5 mm	1.31	1.56	0.25	19.25
DA	0-1 mm	0.53	0.48	0.05	8.88
	1-2 mm	0.56	0.53	0.04	6.34
	2-3 mm	0.57	0.54	0.04	6.47
	3-4 mm	0.58	0.55	0.03	5.05
	4-5 mm	0.59	0.57	0.02	3.87

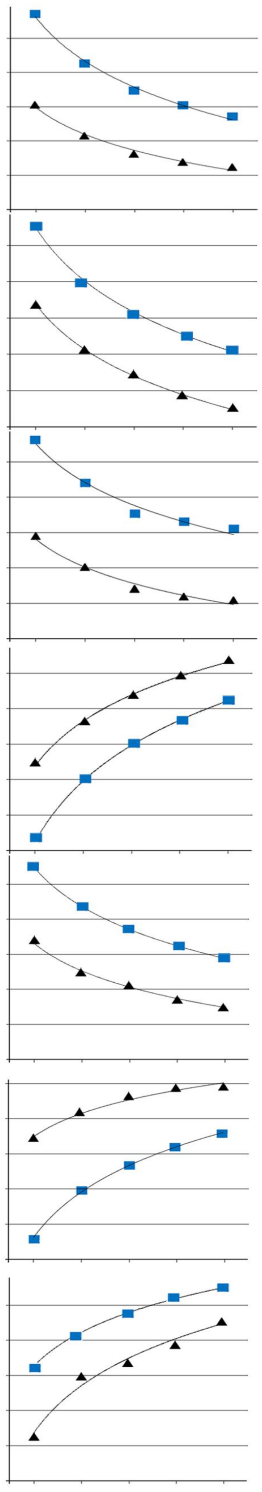

Table 1 Measurements of trabecular bone for healthy and OA patellae for the first 5 mms beneath the subchondral bone plate. (Absolut diff. – difference of greatest and smallest value; % – percentage of the absolute diff. to the healthy measured value)